Research Square

Preprints are preliminary reports that have not undergone peer review.
They should not be considered conclusive, used to inform clinical practice,
or referenced by the media as validated information.

Efficient Fabrication of Cd-Doped NiO Nanostructures as High-Performance Electrode Materials for Supercapacitors

C. Kathiravan
Muthayammal Engineering College, (Autonomous)
K. Balachandran
balanano06@gmail.com
Vivekanandha College of Engineeringfor Women
J. Venkatesan
Muthayammal Engineering College
A. Mani
Muthayammal Engineering College

Research Article

Keywords: Solgel Method, Nano particles, XRD, SEM, Super Capacitor

Posted Date: April 15th, 2026

DOI: https://doi.org/10.21203/rs.3.rs-9188977/v1

License: This work is licensed under a Creative Commons Attribution 4.0 International License.
Read Full License

Additional Declarations: No competing interests reported.

Version of Record: A version of this preprint was published at Journal of Materials Science: Materials in Electronics on April 22nd, 2026. See the published version at https://doi.org/10.1007/s10854-026-17303-y.

Efficient Fabrication of Cd-Doped NiO Nanostructures as High-Performance Electrode Materials for Supercapacitors

C. Kathiravan[a], K. Balachandran[b], J. Venkatesan[c], A. Mani[c].

[a)]Department of Chemistry, Muthayammal Engineering College, Rasipuram, Namakkal, India.

[b)]Department of Chemistry, Vivekanandha College of Engineeringfor Women, Tiruchengode, Namakkal, India.

[c)]Department of Physics, Muthayammal Engineering College, Rasipuram, Namakkal, India.

Corresponding author: balanano06@gmail.com

Abstract

Pure and cadmium-doped NiO nanostructured porous materials, including various concentrations were successfully synthesized via a solvothermal approach consuming citric acid as a hydrolysis-regulating substance and evaluated for supercapacitor applications. Powder X-ray diffraction was employed to examine the phase composition of nanomaterials. The typical crystallite size of the oxide samples ranged from 21 to 9 nm. Fourier transform infrared spectroscopy established the presence of M-O bonding. Morphological investigations revealed a mesoporous, flake-like building in the prepared materials. Energy-dispersive X-ray spectroscopy were used to find out the oxidation states and elemental composition, respectively. Electrochemical performance was analyzed in an aqueous electrolyte using cyclic voltammetry, galvanostatic charge–discharge, and electrochemical impedance spectroscopy. Among the four electrodes, Cd-Nickel-oxides (X=10%) exhibited the maximum surface redox activity and brought a superior specific capacitance of 832 F g^{-1} at a current density of 1 A g^{-1}.

Keywords: Solgel Method, Nano particles, XRD, SEM, Super Capacitor

1. Introduction

Nanotechnology encompasses a wide range of scientific fields, such as microfabrication, molecular engineering, materials science, organic chemistry, molecular biology, and semiconductor physics, largely because of its extremely small scale [1]. Research and applications in this area are equally varied, spanning from advancements in predictable device physics to entirely new strategies based on molecular self-assembly, the development of innovative nanoscale materials, and the precise manipulation of matter at the atomic level. At the same time, nanotechnology raises challenges similar to those associated with other emerging technologies, such as concerns about the environmental effects and toxicity of nanomaterials, their influence on the global economy, and speculation about extreme or catastrophic outcomes. These issues have prompted

discussions among governments and advocacy groups regarding the need for specialized regulations for nanotechnology. Among nanomaterials, transition metal oxide nanoparticles have gained increasing importance for supercapacitor applications [2]. Owing to their nanoscale dimensions, nanoparticles exhibit properties that differ knowingly from those of bulk materials. In particular, nickel oxide nanoparticles with uniform size and good diffusion are highly wanted for use in ceramic, magnetic, electrochromic, and heterogeneous catalytic systems [3]. Various synthesis methods have been reported for producing Nickel-oxides nanoparticles, including sol–gel processes [4], surfactant-assisted methods [5], thermal decomposition [6], polymer-matrix-assisted synthesis [6], and spray pyrolysis [8]. However, several of these approaches face difficulties in achieving uniform particle size and effective dispersion. Electrochemical capacitance has gained significant attention due to its outstanding features, such as high-power density, long-lasting and sustainable energy storage capability, excellent reversibility, prolonged operational life, and minimal maintenance requirements. Supercapacitors also offer higher energy storage capacity than conventional capacitors and are considerably safer compared to batteries [9]. Supercapacitors are usually secret into two types based on their charge storage mechanisms. One category is pseudo capacitors, which store charge through fast Faradaic redox reactions. Materials commonly used in pseudo capacitors include conducting polymers, metal oxides, and metal hydroxides. The other category is electrical double-layer capacitors (EDLCs), which store energy through the electrostatic adsorption of ions at the electrode–electrolyte interface. EDLCs are typically composed of carbon-based materials such as graphene, carbon nanotubes, and activated carbon.

As reported in [10,11], transition metal oxides (TMOs) including TiO_2, V_2O_5, Fe_3O_4, CuO, SnO_2, Bi_2O_3, Nickel-oxides, MnO, ZnO, and Co_3O_4 have attracted considerable interest due to their low cost, environmental compatibility, and comparable electrochemical performance. Among these materials, Nickel-oxides stands out as a promising electrode material for pseudo capacitors because of its high theoretical capacitance (2584 F g^{-1} within a 0.6 V potential window), strong electrochemical activity, abundant redox reactions, eco-friendly nature, affordability, and excellent stability [12]. Owing to these advantages, Nickel-oxides has been widely explored for various applications, including lithium-ion batteries, gas sensors, catalysis, and water treatment adsorption processes [13]. The key properties of nanoparticles, such as particle size, structure, distribution, and morphology, are strongly influenced by the synthesis method employed. Various synthesis techniques, including electrochemical routes, hydrothermal reactions, and precipitation methods, have

been widely developed for the production of nanoparticles (NPs). Among these, the sol–gel method was selected for this study due to its easiness, low cost, and ease of comparison with other fabrication approaches. This technique allows nanoparticle formation at relatively low temperatures while offering effective control over particle size and composition.

The foremost objective of this work is to examine Nickel-oxides nanoparticles doped with Cd^{2+} ions at a concentration of 0.02 M%. With the quick expansion of the electric vehicle industry in current years, supercapacitors have gained considerable attention [14]. To achieve enhanced pseudocapacitive performance, it is essential to design electroactive materials with optimized structures and geometries that maximize surface area utilization and incorporate well-defined porous networks [15]. Previous studies have demonstrated that employing nanostructured electrode materials with diverse Nickel-oxides morphologies—such as nano particles, nano flowers, nano sheets, and nano wires—significantly increases the accessible superficial area of the electrodes [16]. Recent progress in nanoscience and nanotechnology has further enabled the development of nanostructured electroactive materials with improved surface properties, thereby advancing their application in high-performance supercapacitors.

A number of methods, including homogeneous precipitation [17], hydrothermal [18] and micro-wave-assisted homogeneous precipitation [19], can be used to create α & β nickel hydroxides, or diverse phases of α & β nickel hydroxides samples in the presence of cinnamic acid (pH stays comparatively low for the duration of the process). Among these, a simple hydrothermal method is beneficial for producing Nickel-oxides nanoflakes because it requires less equipment, minimal external energy consumption, and cheap precursors. Here, we used a simple hydrothermal method to create undoped and Cd2+ doped diverse phases of α- and β-nickel hydroxide samples cinnamic acid used as a hydrolysis adaptable agent [20].

Pure NiO and cadmium doped NiO nanoparticles were produced by further calcining nickel hydroxide precursors. As a result, the present study makes clear that this solgel process is perfect for creating well-crystalline NiO nanoparticles with intriguing characteristics for application in devices that store electrochemical energy such as supercapacitors. This study used skeletal, internal structure, galvanostatic cycling, elemental, cyclic voltametric, and electrochemical impedance spectroscopic analyses to show the effects of Cd^{2+} at various concentrations on the pseudo capacitive performances of electro active mesoporous nickel-oxides electrodes are ability to conduct electricity.

2. Materials and Synthesis Methodology:

Metal (Cd-NiO) nanoparticles were produced by the sol-gel process, which is a popular and economical way to make metal oxide nanoparticles. In the present study, an aqueous solution containing a known amount of precursor materials, such as nickelous acetate ($Ni(CH_3CO_2)_2 \cdot 4H_2O$) and dopant $CdCl_2.2.5H_2O$ was dissolved in deionized water. First, add 50 ml of distilled water and 100 ml of 2-methoxy-1-ethanol poured together in a beaker. After adding nickelous acetate and cadmium chloride (X= 0, 2.5, 5, 10%), the mixture was constantly agitated for 20 minutes at 80°C with a magnetic stirrer. Citric acid was added dropwise after the nickelous acetate had dissolved while stirring, creating a transparent solution. The green solid precipitate was extensively cleaned with deionized water many times before being eventually cleaned with the proper amount of ethanol. The synthesised products were manually ground for 20 minutes in an agate mortar after being dried for approximately 10 hours at 80 °C on a hot plate. To get Cd doped NiO nanocrystalline products, the greenish products obtained were slowly heated at a speed of 10 °C per minute from ambient temperature to 450 °C and subjected to calcination for 2 hours in an air environment using an electronic furnace. Subsequently, the products turned black in colour. The produced nanoparticles as shown in the Fig. 1.

3. Results and Discussion

3.1 X-ray diffraction analysis:

The XRD patterns of pure Nickel-oxides (x = 0) and Cd-doped Nickel-oxides nanoparticles with Cd concentrations of x = 0%, 2.5%, 5%, and 10% authorize the formation of a single-phase face-centered cubic (fcc) NiO structure. The prominent diffraction peaks appearing at 2θ values of approximately 37.2°, 43.3°, 62.9°, 75.4°, and 79.4° correspond to the (111), (200), (220), (311), and (222) crystallographic planes of Nickel-oxides, respectively (JCPDS No. 47-1049), indicating good crystallinity of all samples. No additional diffraction peaks related to Cd, CdO, or other impurity phases are observed for the Cd-doped samples (x = 0%, 2.5, 5, and 10%), suggesting the fruitful incorporation of Cd^{2+} ions into the NiO lattice without altering the host crystal structure as shown in Fig. 2. A slight shift of the diffraction peaks toward lower 2θ values is observed with growing Cd content, which can be ascribed to lattice expansion caused by the substitution of Ni^{2+} ions (ionic radius 0.69 Å) with larger Cd^{2+} ions (0.95 Å). Furthermore, a noticeable broadening of the diffraction peaks occurs as the Cd concentration increases from x = 0 to x = 10%, indicating a gradual reduction in crystallite size. The crystallite

size, estimated using the Debye–Scherrer equation, shows a systematic decrease for the Cd-doped samples compared to pure Nickel-oxides. Among the four compositions, the 10% Cd-doped Nickel-oxides sample exhibits the smallest crystallite size, which is attributed to increased lattice distortion and strain induced by higher Cd incorporation, effectively suppressing grain growth during nanoparticle formation.These results demonstrate that Cd doping effectively tailors the crystallite size of Nickel-oxides nanoparticles while preserving the cubic crystal structure, making Cd-doped Nickel-oxides a promising material for size-dependent functional applications [21]. The regular crystallite size (D) was calculated from the most intense diffraction peak using the Debye–Scherrer equation:

$$D = \frac{k\lambda}{\beta \cos\theta} \quad (1)$$

3.2 FT-IR spectroscopy analysis:

Fourier transform infrared spectroscopy is extensively applied to recognize functional groups in materials and to study their corresponding vibrational modes. Fig.3-presents the FTIR spectrum of nickel oxide nanoparticles, displaying a number of distinct absorption peaks within the 450–4000 cm^{-1} range. naturally, metal oxides show M-O stretching vibrations in 350–450 cm^{-1} region of the spectrum. In present study, prominent absorption bands at 570 cm^{-1} and 450 cm^{-1} are attributed to the stretching vibrations of Ni–O bonds [22]. A minor shift in these bands was observed with increasing Cd concentration, which can be explained by variations in bond length caused by the substitution of Ni^{2+} ions with Cd^{2+} ions. The broad band cantered around 3445 cm^{-1} resembles to O–H stretching vibrations [23,24], whereas the absorption peak at 1643 cm^{-1} is connected with the bending vibrations of water molecules. Furthermore, the band at 1386cm^{-1} is assigned to C–O bond vibrations [25,26]. The characteristic peaks at 450 and 557 cm^{-1} further confirm the formation of NiO.

3.3. FE-SEM Studies:

The external morphology and elemental composition of the sol–gel–synthesized samples with varying concentrations of dopant were investigated via scanning electron microscopy and energy-dispersive X-ray analysis, with undoped Nickel-oxides serving as a reference. As shown in Fig. 4(a–d), all synthesized samples consist of nearly spherical nanoparticles with a fairly uniform particle size distribution. However, noticeable particle agglomeration is evident, due to larger surface area of small sized nanoparticles. As a result of

strong covalent bond and metallic bond of small sized particles are overlap and combine to aggregates.

The EDAX spectra presented in Fig. 5. reveal the presence of oxygen (O), nickel (Ni), and cadmium (Cd) in the synthesized samples. The detection of cadmium is associated with the reduction of cadmium chloride, while nickel and oxygen originate from the Nickel-oxides lattice. The elemental analysis confirms that the samples exhibit the intended stoichiometric composition, and the EDAX findings further demonstrate the incorporation of Cd into the NiO nanoparticle matrix.

3.4. TEM-Studies:

The interconnected net structure is composed of numerous porous nanowires, which facilitate effective electrolyte penetration and enhance interfacial contact with the electrode material. The TEM images, SAED pattern, and high-resolution (HR-TEM) micrographs of the synthesized Cd–Nickel-oxides nanoparticles are presented in Fig. 6(a-d). The TEM images clearly reveal the uniform dispersion of cadmium (Cd) over the band-like nanostructured materials. In Fig. 6, the dispersed cadmium particles, appearing as dark spherical features on the NiO surface, exhibit an average particle size of approximately 5 nm, while the Nickel-oxides nanoparticles show size distributions in the range of 5–13 nm. The HR-TEM image confirms a lattice spacing of 0.15 nm, corresponding to the (220) crystallographic plane of Nickel-oxides. Furthermore, the selected area electron diffraction (SAED) pattern shown in Fig. 6d indicates the polycrystalline nature of the material, with distinct concentric rings indexed to the (111), (200), and (220) planes, consistent with the prominent peaks observed in the XRD analysis.

3.5. Electrochemical Studies

3.5.1. Cyclic voltammetry:

Using cyclic voltammetry (CV), galvanostatic charge–discharge cycling, and electrochemical impedance spectroscopy (EIS) in a three-electrode configuration with a 3 M KOH aqueous electrolyte, the pseudocapacitive performance of the nanocrystalline oxides was systematically examined. At a scan rate of 5 mV s^{-1}, the CV profiles of pure and doped Nickel-oxides electrodes are displayed in the figure. As illustrated in Fig. 7. all four electrodes exhibit well-defined and regular CV curves. Since the specific capacitance is directly related to the enclosed CV area, these shapes reflect their capacitive behaviour. It is widely recognized that increasing dopant concentration leads to a reduction in the space-charge region and an increase in surface barrier height [27,38], where the strong internal electric field efficiently separates electron–hole pairs prior to recombination. The incorporation of Cd into Nickel-oxides

suppresses nanoparticle agglomeration by lowering the Nickel-oxides phase transition and stabilizing Nickel-oxides species at interparticle contacts. Consequently, Cd^{2+} doping slightly restricts particle growth compared with pristine Nickel-oxides, while leaving the overall morphology unchanged. Moreover, calcination converts hydroxides into oxides, generating a nanoporous architecture. This mesoporous structure enhances utilization of the electroactive material by promoting efficient ion and electron transport during electrochemical cycling, thereby contributing to the overall capacitance. Consequently, a high scan rate causes OH^- to be oversaturated during reduction or rapidly depleted during oxidation. At higher scan rates, when the redox reaction experiences restricted diffusion, both the interfacial reaction kinetics and the ion transfer rate are ineffective. The components of the electrode's surface are inaccessible at rapid charging and discharging rates, and the electrolyte/electrode contact experiences OH^- depletion or oversaturation, which hinders charge transfer and increases resistance. The CV curves for the pure Nickel-oxides electrode in this electrochemical investigation unmistakably show a quasi-rectangular form, demonstrating optimal capacitive behaviour. The kinetic irreversibility of the redox process is responsible for the non-symmetric reduction and oxidation peaks seen in the Cd-doped Nickel-oxides electrodes. Determined by the superficial redox mechanism of Ni^{2+} to Ni^{3+} at the surface of Nickel-oxides compounds, the presence

of these oxidation-reduction peaks during the charging and discharging process indicates a Faradaic pseudocapacitive character [28,36,37]. The oxidation-reduction peaks also shifted to higher and lower potentials at that point, and the scan rate increased from 5 to 200 mV/s.

$$NiO + OH^- = NiOOH + e^-$$

$$Ni(OH)_2 + OH^- = NiO(OH) + H_2O + e^-$$

The electrochemical properties of the Nickel-oxides electrode are significantly enhanced by an alkaline KOH electrolyte, based on the generated CV graphs. This increase is caused by the rapid intercalation and deintercalation of K^+ ions. The Nickel-oxides electrode's areal capacitance (Csp) is significantly increased by the strong conductivity and better ionic transport of potassium ions in the electrolytic solution.

The exact observation of discrete redox peaks in the substances with nanostructures Cd-doped Nickel-oxides (NiO_{1-x}, x = 2.50, 5.0, and 10%) electrodes was ascribed to process of ion or electron transmission.These results demonstrate the exceptional reversibility and high-rate capabilities of the working electrodes [29,39-41].

The following formula is used to calculate the spatial capacitance of Cd-doped and pure nickel-oxides electrodes based on the CV curves.

$$C_{sp} = \frac{1}{v \times m \times \Delta V} \int I(V)dV \quad (3)$$

In this context, m denotes the mass of the active Nickel-oxides material in grams (mg), V represents the scan rate (V s^{-1}), and CS corresponds to the areal capacitance of the electrode material (Fg^{-1}). The potential window applied during measurement is indicated by ΔV (V), while the integral term signifies the area under the CV curve, representing the entire charge involved in the electrochemical process. More precisely, the area below the CV curve over the potential range ΔV is given by ∫I(V)dV, where I (V) is the current response at a particular potential V.

At a scan rate of 5 mV s^{-1}, the estimated areal capacitance (Csp) of the prepared pure and Cd-doped Nickel-oxides electrodes yields ultra capacitance values of 151.9, 159.5, 275.9 and 457 F g^{-1}. Fig. 7 illustrates the effect of scan rate on the areal capacitance (Csp) of pure and Cd-doped NiO1-$_x$ (x = 2.5, 5, and 10%). At lower scan rates, K^+ ions from the electrolyte can more effectively intercalate and deintercalated into the larger active sites of the electrode. A noticeable decrease in Csp with increasing scan rate is observed. This enhanced performance is attributed to the uniform dispersion of fine particles within the electrode material, which facilitates improved ion distribution into the Nickel-oxides structure. As a result, the Cd-doped NiO_{1-x} (x = 10%) electrode demonstrates greater charge capability, Consider the potential of being an ideal choice for ultracapacitor applications. Fig. 8. Shows that uitra capacitance values of Pure and metal (Cd)-doped NiO electrodes at 5 mV/s.

3.5.2. Galvanometric Charge-Discharge Studies:

Galvanostatic charge–discharge (GCD) is a widely employed electrochemical technique for evaluating the charge storage performance and durability of supercapacitor electrodes. In this method, a constant current is applied to the electrode while the potential variation with time is monitored within a defined voltage window. The shape of the charge–discharge curves provide insight into the capacitive behaviour, reversibility, internal resistance, and stability of the electrode material. Capacitance values are quantitatively determined from the discharge profiles, making GCD an essential tool for assessing the practical applicability of supercapacitor materials. To conduct additional assessment of the electrode materials., galvanostatic charge–discharge (GCD) measurements were performed. Fig. 9. presents the charge–discharge profiles of pristine Nickel-oxides and doped nickel-oxides electrodes

recorded at a current density of 2 A g^{-1}. The specific capacitance values of the electrodes were calculated from the GCD curves using Ruoff's equation (Eq. 5).

$$C_{sp} = \frac{I\,\Delta t}{m\,\Delta V} \quad (4)$$

In this equation, m (g) denotes the mass of the electrochemically vigorous material in the working electrode, I (A g^{-1}) denotes the applied discharge current, and ($T_2 - T_1$) corresponds to the discharge time interval during which the electrode potential decreases from the maximum value (Vmax to half of that value) (½Vmax).

Galvanostatic charge–discharge measurements of the Cd:NiO thin films were carried out at different current densities (1, 1.5, 2.0, 2.5, 3.0, 3.5 and 4.0 mA cm^{-2}) in 1 M KOH electrolyte within a potential window of -0.2 to 4.0 V, as shown in Fig. 9(a). The charge–discharge curve recorded at a current density of 1 mA cm^{-2} exhibits a prolonged charge–discharge time compared to the other current densities, reaching the full potential window under constant current operation. The non-linear nature of the discharge curves shown in Fig. 9(b-d) indicates pseudocapacitive behaviour, and the discharge time is observed to gradually decrease with increasing current density. The ultra capacitance values calculated from the discharge curves at current densities of (1, 1.5, 2.0, 2.5, 3.0, 3.5 and 4.0 mA cm^{-2} were 832, 707, 597 and 505 F g^{-1} (X=10 %). The specific capacitance obtained at a low current density of 1 mA cm^{-2} exhibits maximum value due to the longer discharge time.

The observed decrease in specific capacitance with increasing current density is ascribed to the limited utilization of active materials. At higher current densities, only the outer surface of the electrode participates in charge storage, whereas at lower current densities the charge accumulation process is slower, allowing electrolyte ions to access all active sites and porous structures, thereby enhancing the energy storage capability [30, 31,42].

The galvanostatic charge–discharge curves for pure Nickel-oxides were recorded at a current density of 0.4 mA cm^{-2} within a potential window of 0–0.45 V. Fig.10. presents the charge–discharge profiles of undoped and Cd-doped Nickel-oxides electrodes at the same current density. It is evident that the discharge time is significantly increased for the Cd-doped Nickel-oxides electrode compared to the undoped Nickel-oxides, indicating enhanced capacitive performance. However, the operating potential window of the Cd-doped Nickel-oxides electrode is slightly reduced relative to that of pure Nickel-oxides. Fig.10 illustrates the variation of specific capacitance of the Cd-doped Nickel-oxides (x = 10%) electrode as a function of different scan rates and current densities.

Energy density (Ed) and power density (Pd) are fundamental parameters used to evaluate the performance of electrochemical capacitors (ECs). These characteristics were utilized to examine the electrochemical behavior of the asymmetric supercapacitor employing Cd-doped Nickel-oxides electrodes. The average values of energy and power densities were determined using the following expressions [32,33].

$$E_d = \frac{1}{2} C_{sp} \Delta V^2 / 3.6 \quad (5)$$

$$P_d = 3600 / \frac{E_d}{\Delta t} \quad (6)$$

Here, Ed denotes the energy density (Wh kg^{-1}), Csp represents the specific capacitance (F g^{-1}) at a given scan rate, and ΔV^2 corresponds to the operating potential window (V). Pd and Δt^2 refer to the power density and discharge time (s), separately. The energy and power density values achieved at a given current density of 1 A g^{-1} are 25.25 Wh kg^{-1} and 727.20 W/ kg for pure NiO; 29.8 Wh/kg and 864.54 W/kg for NiO_{1-x} (x = 2.5%); 35.35 Wh/kg and 1043 W/kg for NiO_{1-x} (x = 5%); and 46.10 Wh/kg and 1217.56 W/kg for NiO_{1}-X (x = 10%). The energy and power densities were designed at various current densities, and the corresponding values are summarized in Tables 3.

The variation in energy density exhibits an inverse relationship with power density as the current density decreases, indicating a notable swap-off in electrochemical capacitor performance. This opposing trend suggests that an increase in power density enhances the electrode's capability to bring energy at a quick rate, which is openly related to the discharge current [32,33,].

3.5.3 Electrochemical Impedance Spectroscopy:

Electrochemical Impedance Spectroscopy (EIS) is a powerful diagnostic tool for evaluating the charge transfer behavior, ion diffusion kinetics, and interfacial characteristics of electrode materials intended for high-performance supercapacitor applications. The impedance response is commonly represented by a Nyquist plot, where the imaginary part of impedance (Z'') is plotted against the real part (Z') across a broad frequency range. For an efficient supercapacitor electrode, the Nyquist plot typically displays a small or negligible semicircle in the high-frequency region, indicating low charge transfer resistance (Rct) and high electrical conductivity at the electrode–electrolyte interface. The intercept of the Nyquist curve with the real axis at high frequency corresponds to the equivalent series resistance (ESR), which

includes contributions from the electrolyte, electrode material, and current collector. A lower ESR is highly desirable, as it ensures minimal energy loss and improved power density.

In the low-frequency region, an almost vertical straight line is observed for ideal capacitive behavior, reflecting rapid ion diffusion and efficient electrolyte access to the electrochemically active sites within the electrode structure. The presence of a short Warburg region or a steeper low-frequency slope indicates reduced ion diffusion resistance, which is critical for fast charge–discharge processes

In the Nyquist plot, the semicircular region corresponds to the charge transfer resistance (Rct) and the double-layer capacitance at the electrode/electrolyte interface, whereas the linear region at low frequencies represents the Warburg impedance related to ion diffusion within the electrode material [33]. The intercept of the impedance curve with the real axis indicates the intrinsic series resistance (Rs), which includes aids from the electrolyte, electrode material, and interfacial contact resistance. The Nyquist analysis reveals (Rct) values of 0.53, 0.52, 0.01, and 4.32 Ω for the undoped & Cd-doped NiO electrodes, respectively, while the corresponding (Rs) values are 3.2, 3.3, 3.4, 3.6, and 1.6 Ω. As shown in the Fig. 11.

The relatively low-Rs and low-Rct values demonstrate enhanced electro chemical performance and faster charge–discharge behavior, representing effective electron transport and rapid charge transfer at the electrode/electrolyte interface [34,35,42]. Overall, a Nyquist plot characterized by low ESR, small charge transfer resistance, and a near-vertical line in the low-frequency domain signifies superior electrochemical kinetics and enhanced ion transport. These features collectively contribute to improved capacitance, high rate capability, and long-term cycling stability, making the electrode material highly suitable for advanced supercapacitor applications.

Conclusion

In this study, we confirmed the successful synthesis of porous-structured Nickel-oxides nanoparticles using a solvothermal method, where Nickel-oxides was employed as the precursor and a cadmium salt was introduced as the dopant. The electrochemical performance of the resulting Cd-doped nickel-oxide nanoparticles demonstrated a high specific capacitance of up to 832 F g^{-1} and also gives maximum power density 1217.6 $KWkg^{-1}$ which is significantly greater when compared to other metal-doped Nickel-oxides nanoparticles. As a result, such nanoparticles exhibit enhanced electrochemical properties and show strong potential as efficient electrode materials in nanoparticle-based energy storage applications.

References:

[1] J. Bahadur, D. Sen., S. Mazumder, S. Ramanathan, J. Sol.Sta. Chem., Vol. 181, 2008, pp. 1227–1235.

[2] Feldmann, C. and Jungk, H.O., 2001. Polyol-mediated preparation of nanoscale oxide particles. Angewandte Chemie (International ed. in English), 40(2), pp.359-362.

[3] Tao, D. and Wei, F., 2004. New procedure towards size-homogeneous and well-dispersed nickel oxide nanoparticles of 30 nm. Materials Letters, 58(25), pp.3226-3228.

[4] Liu, K.C. and Anderson, M.A., 1996. Porous nickel oxide/nickel films for electrochemical capacitors. Journal of the Electrochemical Society, 143(1), pp.124-130.

[5] Wang, Y.D., Ma, C.L., Sun, X.D. and Li, H.D., 2002. Preparation of nanocrystalline metal oxide powders with the surfactant-mediated method. Inorganic Chemistry Communications, 5(10), pp.751-755.

[6] Xiang, L., Deng, X.Y. and Jin, Y., 2002. Experimental study on synthesis of NiO nano-particles. Scripta Materialia, 47(4), pp.219-224.

[7] Deki, S., Yanagimoto, H., Hiraoka, S., Akamatsu, K. and Gotoh, K., 2003. NH2-terminated poly (ethylene oxide) containing nanosized NiO particles: synthesis, characterization, and structural considerations. *Chemistry of materials*, *15*(26), pp.4916-4922.

[8] Liu, S.F., Wu, C.Y. and Han, X.Z., 2003. Preparation of nanoscale nio powders by polymer-network gel process. Chinese Journal of Inorganic Chemistry, 19(6), pp.624-626.

[9] D. Han, P. Xu, X. Jing, J. Wang, D. Song, J. Liu, M. Zhang, Facile approach to prepare hollow core–shell NiO microspherers for supercapacitor electrodes, J. Solid State Chem. 203 (2013) 60–67.

[10] Liuyang Zhang, Pengfei Cai, Zhihao Wei, Tao Liu, Jiaguo Yu, Ahmed A. AlGhamdi, S. Wageh, Synthesis of reduced graphene oxide supported nickelcobalt-layered double hydroxide nanosheets for supercapacitors, Journal of Colloid and Interface Science, 558 (2021) 637-645.

[11]Venkatesan, J., Franklin, J.B., Fathima, J.P.R., Maadeswaran, P., Kaviyarasu, K. and Sundaram, S.J., 2026. Synergistic effect of biomass-derived activated carbon with Zn-Bi2O3 nanocomposite for high-performance supercapacitor electrodes. *Ionics*, pp.1-18.

[12] G. Bharathy, P., Raji Room temperature ferromagnetic behavior of Mn-doped NiO nanoparticles: a suitable electrode material for supercapacitors, J. Mater. Sci.: Mater. Electron. 28 (2017) 17889–17895.

[13] B.G.S. Raj, B. Natesan, A.M. Asiri, J.J. Wu, S. Anandan, Pseudocapacitive properties of nickel oxide nanoparticles synthesized via ultrasonication approach, ionic 26 (2020) 953–960

[14] Chen, J.; Huang, Y.; Li, C.; Chen, X.; Zhang, X. Synthesis of NiO@MnO2 core/shell nanocomposites for supercapacitor application. Appl. Surf. Sci. 2016, 360, 534−539.

[15] Kasavajjula, U.; Wang, C.; Appleby, A. J. Nano- and Bulk Silicon-Based Insertion Anodes for Lithium-Ion Secondary Cells. J.Power Sources 2007, 163, 1003−1039.

[16] Lee, J. H.; Lim, J. Y.; Lee, C. S.; Park, J. T.; Kim, J. H. Direct growth of NiO nanosheets on mesoporous TiN film for energy storage devices. Appl. Surf. Sci. 2017, 420, 849−857.

[17] Zhao, Y. L.; Wang, J. M.; Chen, H.; Pan, T.; Zhang, J. Q.; Cao, C. N. Al-Substituted α-Nickel Hydroxide Prepared by Homogeneous Precipitation Method with Urea. Int. J. Hydrogen Energy 2004, 29,889−896.

[18] Zheng, Y. Z.; Ding, H. Y.; Zhang, M. L. Preparation and Electrochemical Properties of Nickel Oxide as a Supercapacitor Electrode Material. Mater. Res. Bull. 2009, 44, 403−407.

[19] Meher, S. K.; Justin, P.; Rao, G. R. Microwave-Mediated Synthesis for Improved Morphology and Pseudocapacitance Performance of Nickel Oxide. ACS Appl. Mater. Interfaces 2011, 3, 2063−2073.

[20] Xing, W.; Li, F.; Yan, Z. F.; Lu, G. Q. Synthesis and Electrochemical Properties of Mesoporous Nickel Oxide. J. Power Sources 2004, 134, 324−330.

[21] Alshahrie, A., Yahia, I.S., Alghamdi, A. and Al Hassan, P.Z., 2016. Morphological, structural and optical dispersion parameters of Cd-doped NiO nanostructure thin film. Optik, 127(12), pp.5105-5109.

[22] Duraisamy, N., Numan, A., Fatin, S. O., Ramesh, K., & Ramesh, S. (2016). Facile sonochemical synthesis of nanostructured NiO with different particle sizes and its electrochemical properties for supercapacitor application. Journal of colloid and interface science, 471, 136-144.

[23] Venkatesan, J., Franklin, J.B., Fathima, J.P.R., Sundaram, S.J., Vasanthi, G. and Kaviyarasu, K., 2025. Biomass waste-derived activated carbon modified with nickel-doped α-Bi2O3 for high-performance supercapacitor electrodes. *Ionics*, *31*(11), pp.12197-12212.

[24] Venkatesan, J., Kumar, J.V., Ragulkumar, E., Franklin, J.B., Sundaram, S.J., Alam, M.W. and Sadaf, S., 2025. Tailoring graphitic carbon nitride properties through shock wave engineering: a path to enhanced optical and structural performance. *Journal of Materials Science: Materials in Electronics*, *36*(21), p.1347.

[25] Ahmad, W., Bhatt, S. C., Verma, M., Kumar, V., & Kim, H. (2022). A review on current trends in the green synthesis of nickel oxide nanoparticles, characterizations, and their applications. Environmental Nanotechnology, Monitoring & Management, 18, 100674.

[26] Franklin, J.B., Paul, J.F.J., Venkatesan, J., Harini, S., Fathima, J.P.R., Sundaram, S.J. and Kaviyarasu, K., 2025. Biomass-derived activated carbon and ZnCo2O4 nanoparticles for high-performance supercapacitors. *International Journal of Electrochemical Science*, p.101172.

[27] Wang, H., Yi, H., Chen, X., & Wang, X. (2013). Facile synthesis of a nano-structured nickel oxide electrode with outstanding pseudocapacitive properties. Electrochimica Acta, 105, 353-361.

[28] Sharma, R., & Yadav, K. (2018). Effect of lattice defects on the structural and optical properties of Ni1− X Ag XO (where X= 0.0, 0.01, 0.03, 0.05, 0.10 and 0.15) nanoparticles. Applied Physics A, 124(2), 88.

[29] Alem, A. F., Worku, A. K., Ayele, D. W., Wubieneh, T. A., abebawTeshager, A., Admasu, B. T., ... &Yemata, T. A. (2023). Ag doped Co3O4 nanoparticles for high-performance supercapacitor application. Heliyon, 9(2).

[30] M. Huang, Y. Zhang, F. Li, L. Zhang, Z. Wen, Q. Liu, Facile synthesis of hierarchical Co3O4@MnO2 core–shell arrays on Ni foam for asymmetric supercapacitors, J. Power Sources 252 (2014) 98–106.

[31] X. Zhang, P. Yu, H. Zhang, D. Zhang, X. Sun, Y. Ma, Rapid hydrothermal synthesis of hierarchical nanostructures assembled from ultrathin birnessitetype MnO2 nanosheets for supercapacitor applications, Electrochim. Acta 89 (2013) 523–529.

[32] Iqbal, J., Numan, A., Omaish Ansari, M., Jafer, R., Jagadish, P. R., Bashir, S., ... & Ramesh, S. (2020). Cobalt oxide nanograins and silver nanoparticles decorated fibrous

polyaniline nanocomposite as battery-type electrode for high performance supercapattery. Polymers, 12(12), 2816.

[33] Kathiravan, C., Balachandran, K., Infantiya, S.G. and Karthikeyan, S., 2026. Facile fabrication of Ag-doped NiO nanostructures as a potential electrode material for enhanced supercapacitor applications. Journal of Materials Science: Materials in Electronics, 37(1), p.4.

[34] Xu, J., Liu, Y., He, L., Zhang, C., & Zhang, Y. (2016). Facile synthesis of CuO mesocrystal/MWCNT composites as anode materials for high areal capacity lithium ion batteries. Ceramics International, 42(10), 12027-12032.

[35] Britto, J. F., Samson, V. A. F., Bernadsha, S. B., Madhavan, J., & Raj, M. V. A. (2022). Synthesis of rNiCo nanocomposite-as an electrode material for supercapacitor applications. Journal of Inorganic and Organometallic Polymers and Materials, 32(12), 4601-4613.

[36] Yi, T.F., Mei, J., Guan, B., Cui, P., Luo, S., Xie, Y. and Liu, Y., 2020. Construction of spherical NiO@ MnO2 with core-shell structure obtained by depositing MnO2 nanoparticles on NiO nanosheets for high-performance supercapacitor. Ceramics International, 46(1), pp.421-429.

[37] Park, H.W., Na, B.K., Cho, B.W., Park, S.M. and Roh, K.C., 2013. Influence of vanadium doping on the electrochemical performance of nickel oxide in supercapacitors. Physical Chemistry Chemical Physics, 15(40), pp.17626-17635.

[38] Akumarti, R., Vangapandu, A., Gattupalli, M.R., Budithi, R.K., K, S. and Rotte, N.K., 2026. Easy synthesis and multifunctional analysis of ZnO, NiO, and ZnO/NiO nanomaterials for enhanced photoluminescence and supercapacitor performance. *Ionics*, pp.1-14.

[39] Fang, Y., Chen, X., Kang, S., Liu, J., Cui, L. and Zhang, J., 2021. Facile template-free synthesis of mesoporous cobalt sulfide for high-performance hybrid supercapacitors. *Journal of Materials Science: Materials in Electronics*, *32*(24), pp.28663-28673.

[40] Mallick, P., Moharana, S., Biswal, L. and Satpathy, S.K., 2023. Transition metal oxide-based nanomaterials for advanced energy storage. In *Emerging Nanodielectric Materials for Energy Storage: From Bench to Field* (pp. 331-355). Cham: Springer International Publishing.

[41] Zemieche, A., Chetibi, L., Hamana, D., Achour, S. and Noto, V.D., 2024. Symmetric and asymmetric supercapacitor fabrication based on green synthesized NiO nanoparticles and graphene. *Colloid Journal*, *86*(2), pp.330-345.

[42] Venkatesan, J., Fathima, J.P.R., Franklin, J.B., Padmanaban, A., Kumaresan, A., Sundaram, S.J., Maadeswaran, P. and Kaviyarasu, K., 2026. Interface-engineered CuBi2O4/biomass-derived activated carbon composites for supercapacitors. *Biomass and Bioenergy*, *211*, p.109223.

Figure Captions Cd-NiO

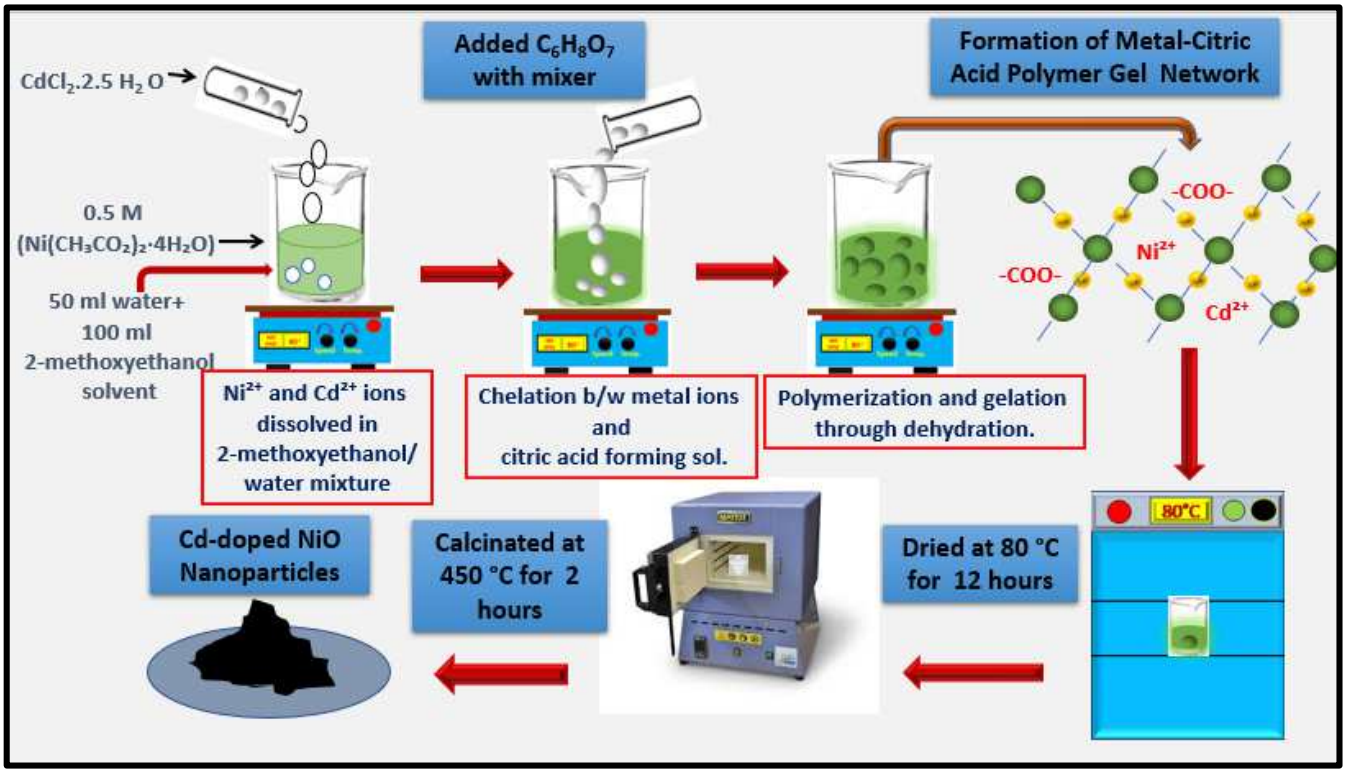


Fig. 1. A schematic representation of the synthesis procedure for Cd-doped NiO nanoparticles using the sol-gel method

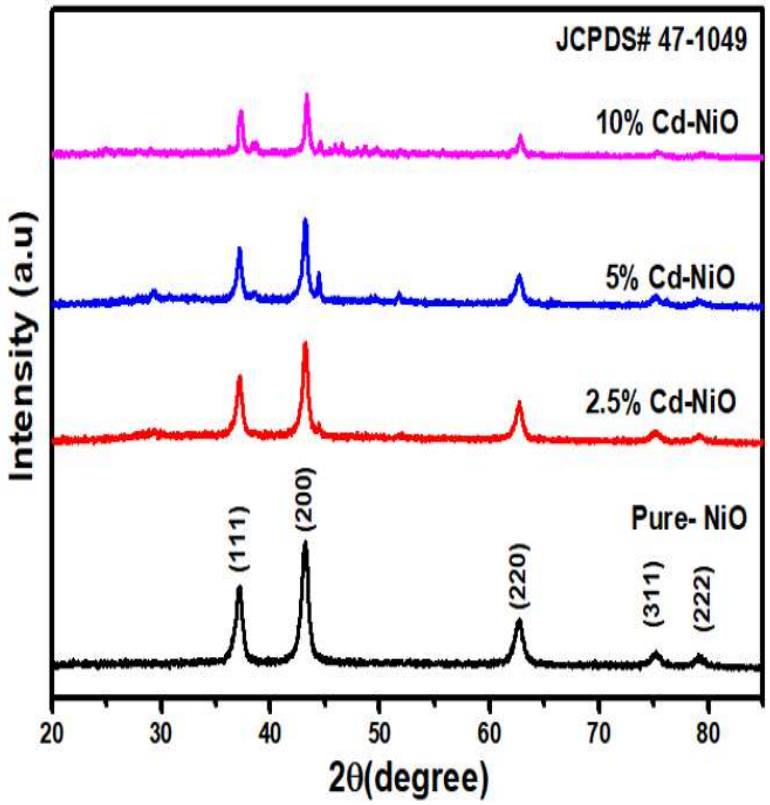


Fig. 2. shows the XRD peaks for pure and Cd-doped NiO nanoparticles.

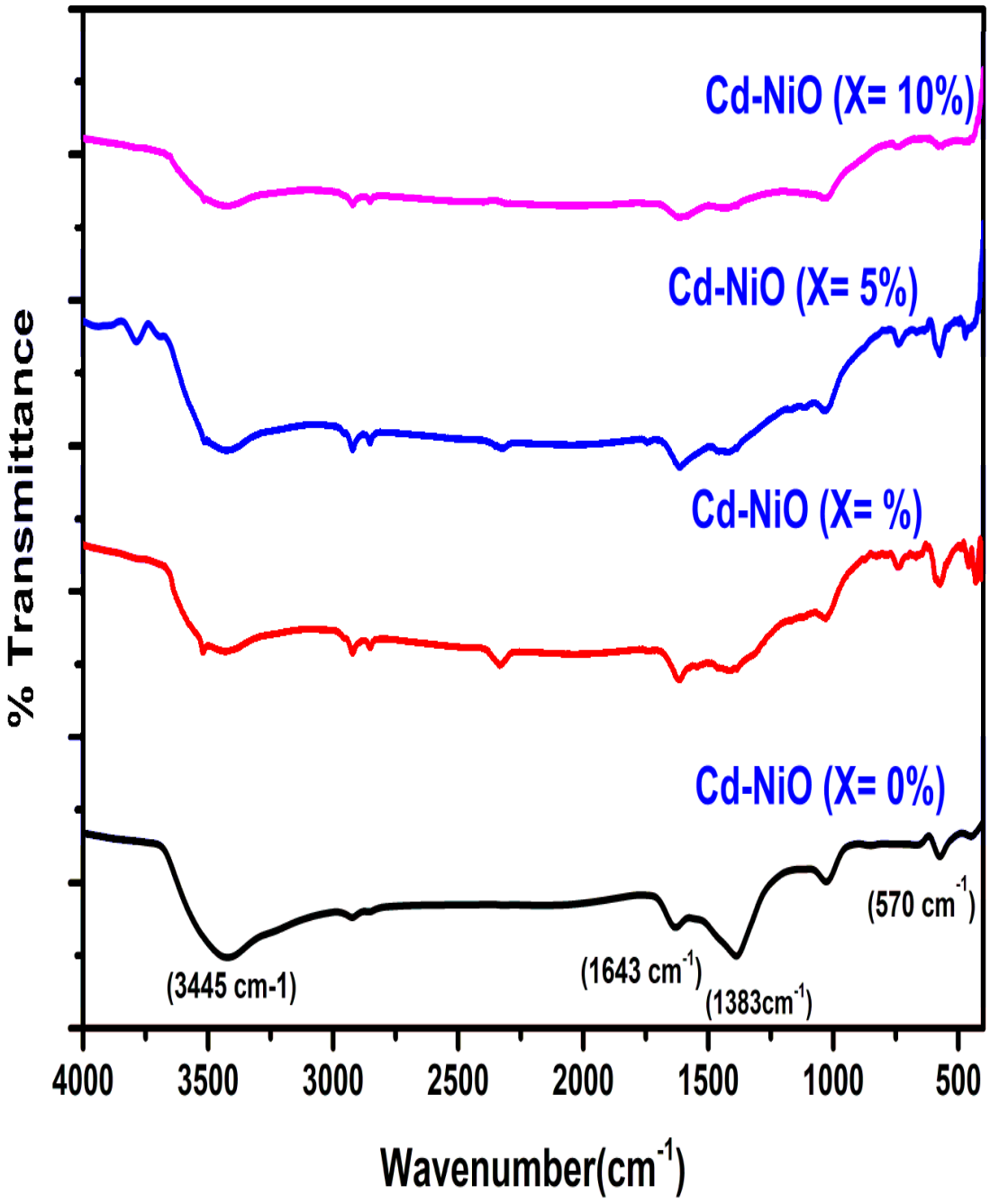


Fig. 3 FT-IR spectra of Pure and Cd-doped NiO Nanoparticles

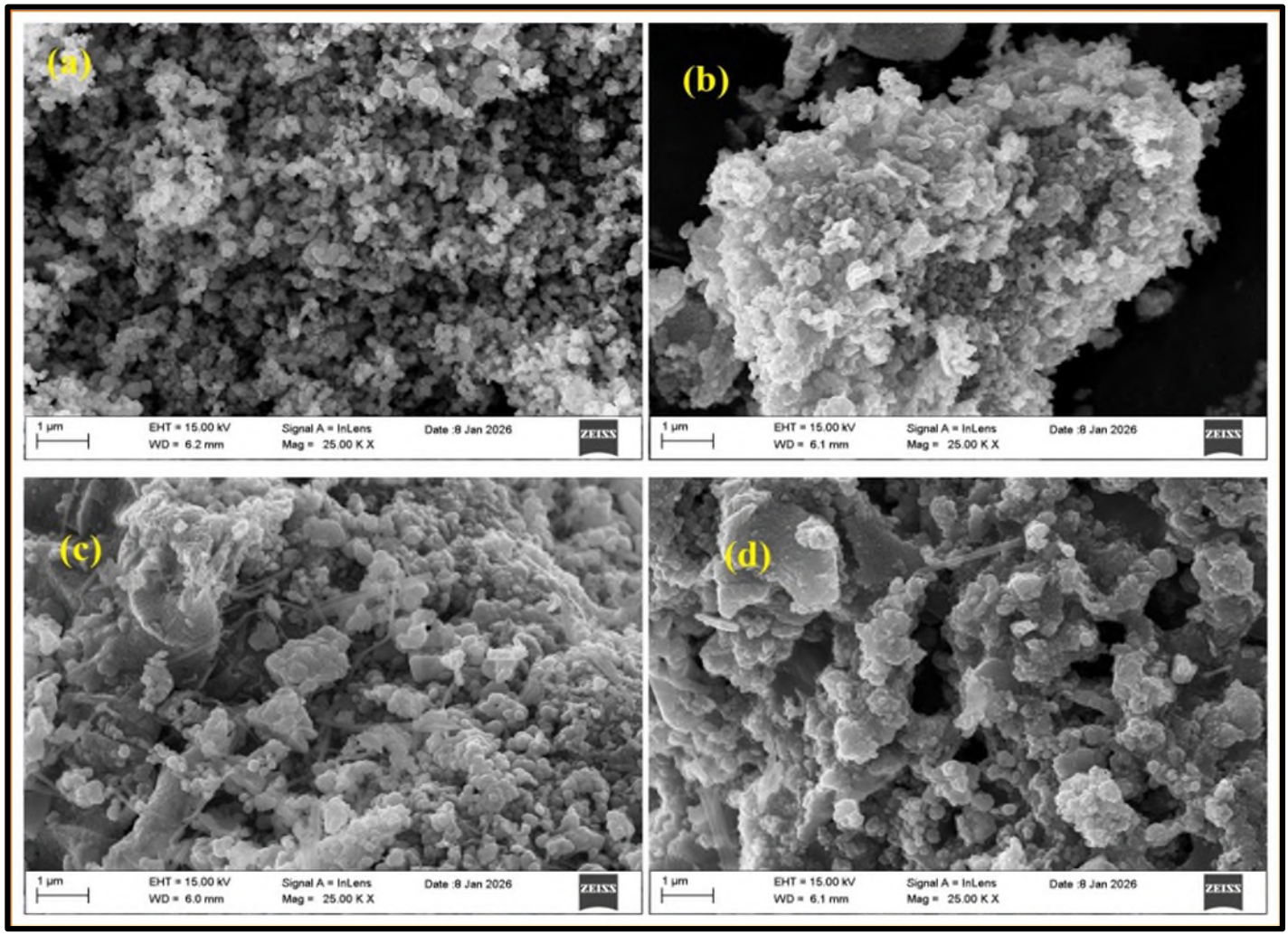


Fig. 4 (a-d) Surface Topography of Pure and Cd-doped NiO Nanoparticles

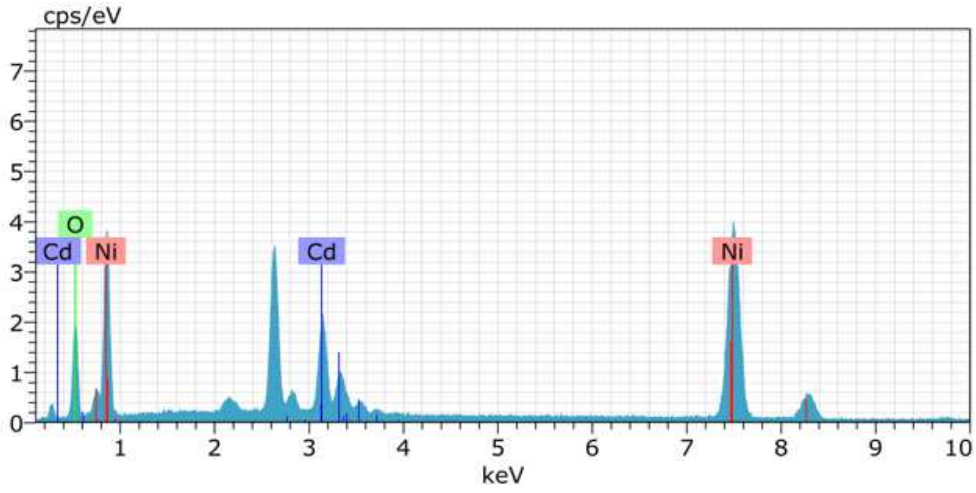


Fig. 5 EDAX Spectra of Cd-doped NiO Nanoparticles

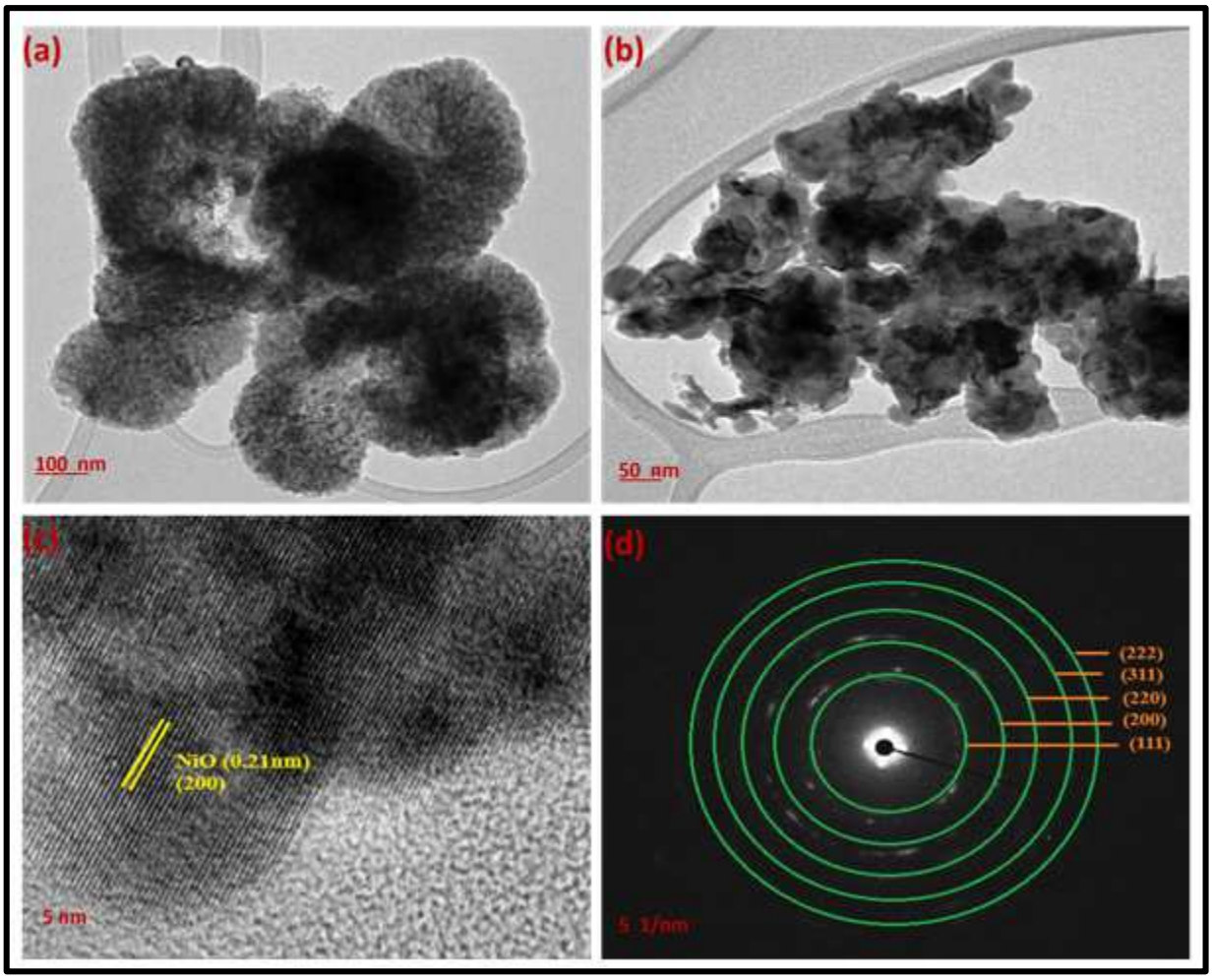


Fig. 6 TEM images (a,b), HR-TEM images (c) and SAED pattern(d) of Cd-NiO nanomaterials

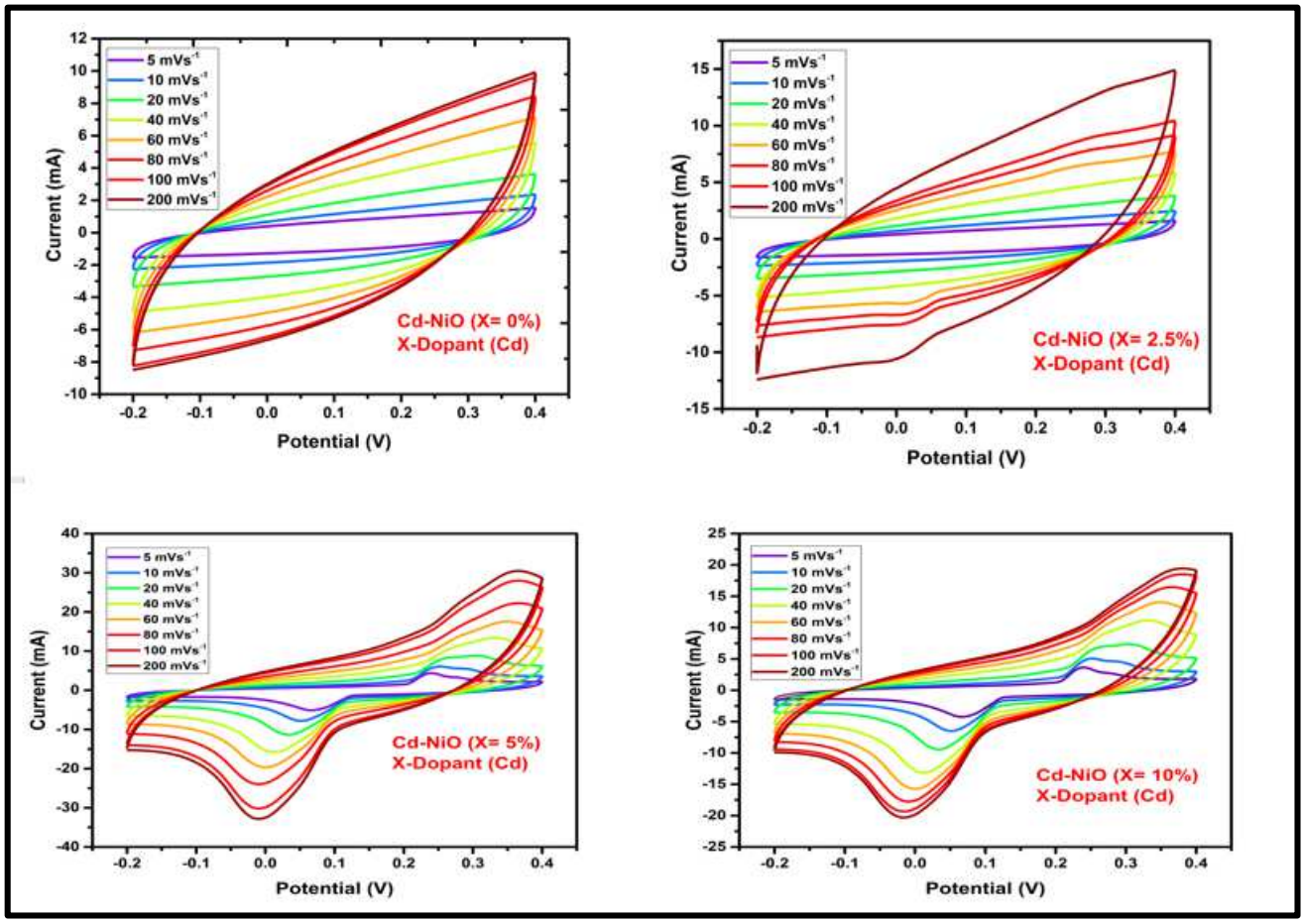


Fig. 7 Cyclic Voltammetry Profiles of Pure and Cd-doped NiO at the scan rate of 5 to 200 mV/s

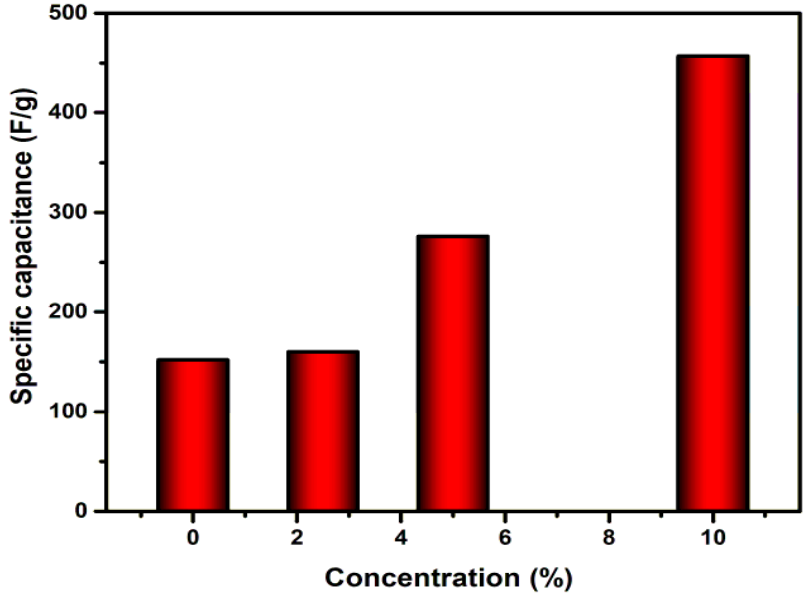


Fig. 8 Specific capacitance values of Pure and Cd-doped NiO electrodes at 5 mV/s.

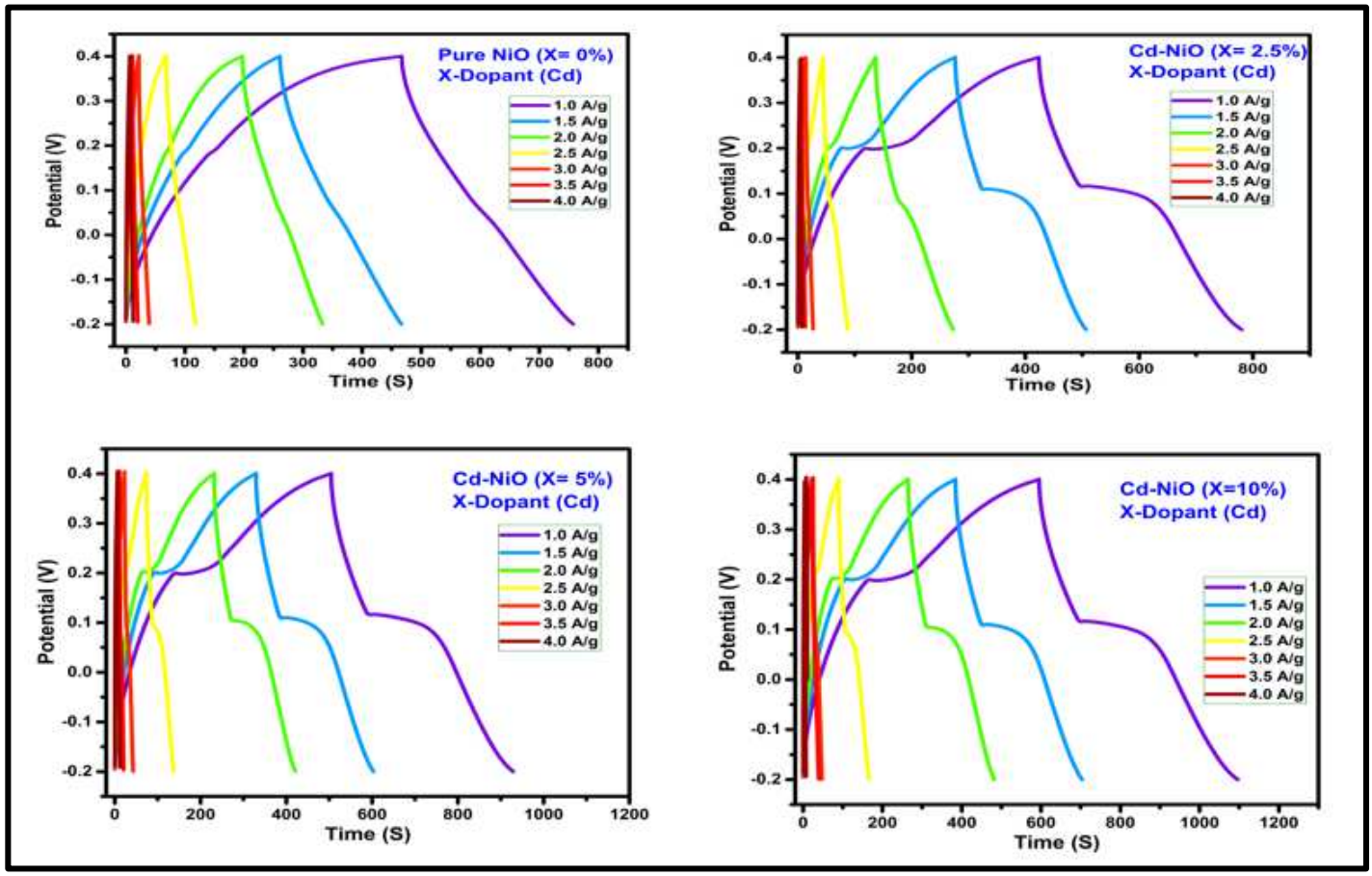


Fig. 9 GCD Profiles of Pure and Cd-doped NiO at the various current densities

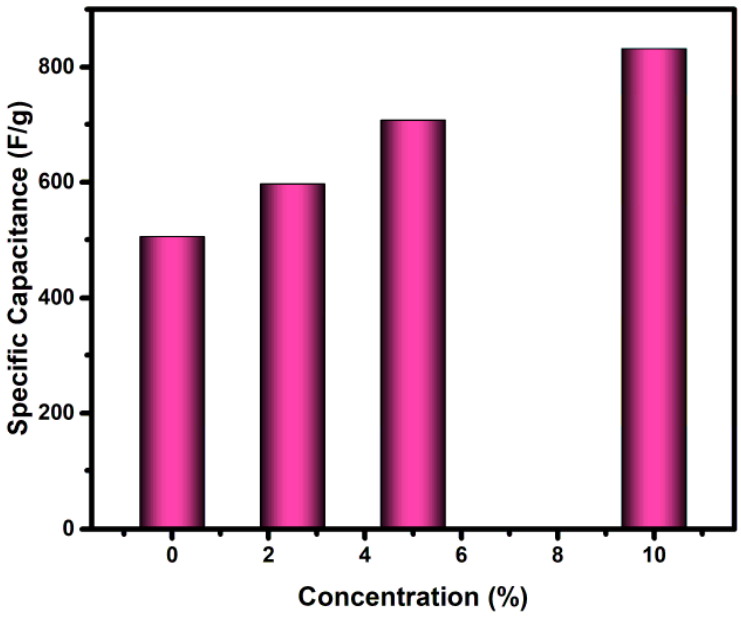


Fig. 10 Comparison of specific capacitance values of Pure and Cd-doped NiO electrodes from galvanostatic charge -discharge

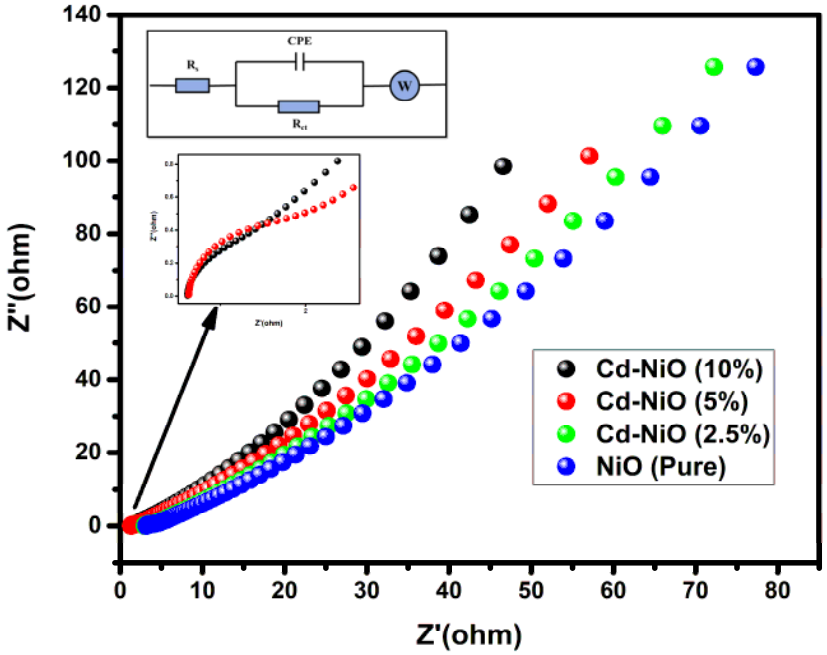


Fig. 11 Nyquist plot of pure and Cd-doped NiO nanoparticles

Table 1. Crystallite size of Cd-doped NiO nanoparticles

Cd concentration (x %)	FWHM (rad)	Crystallite size D (nm)
0 (Pure NiO)	0.4606	~28
2.5	0.5207	~22
5	0.7805	~17
10	1.1353	~12

Table 2. Elemental Analysis of Cd-Doped Nickel Oxide Nanoparticles.

El	AN	unn. C [wt.%]	norm. C [wt.%]	Atom. C [at.%]	Sigma) [wt.%]
Ni	28	50.02	68.76	50.62	1.38
O	8	11.74	16.13	43.57	1.73
Cd	48	10.99	15.10	5.81	0.37
Total		**72.74**	**100.00**	**100.00**	

Table 3.

Energy density (Wh kg^{-1}) and power density (kW kg^{-1}) of pure and Cd-doped NiO electrodes at different current densities

Sample	Energy Density ($Whkg^{-1}$)				Power Density ($KWkg^{-1}$)			
	1 Ag^{-1}	**2 Ag^{-1}**	**3 Ag^{-1}**	**4 Ag^{-1}**	**1 Ag^{-1}**	**2 Ag^{-1}**	**3 Ag^{-1}**	**4 Ag^{-1}**
Pure	25.25	23.5	22.5	10	727.20	2286.48	6934.93	7468.88
X = 2.5%	29.8	28.75	23.65	13.75	864.54	2723.68	7352.34	8519.78
X = 5%	35.35	38.65	32.75	27.7	1043.12	3235.82	8403.42	13907.90
X = 10%	41.6	40.4	35.5	28.5	1217.56	3195.78	8052.92	12272.72